Tethered Power Supply for Quadcopters: Architecture, Analysis and Experiments

Karan P. Jain*, Prasanth Kotaru*, Massimiliano de Sa, Mark W. Mueller†, and Koushil Sreenath†

***Abstract*— Tethered quadcopters are used for extended flight operations where the necessary power to the system is provided through the tether from an external power source on the ground. In this work, we study the design factors such as the tether mass, electrical resistance, voltage conversion efficiency, etc. that influence the power requirements. We present analytical formulations to predict the power requirement for a given setup. Additionally, we show the existence of a critical hover height for a single-quadcopter tether system, beyond which it is physically (electrically) impossible for the quadcopter to hover due to the increasing mass of the tether load and any additional current increasing resistive losses instead of getting delivered to the quadcopter. We then present experimental results for single quadcopter tethered system and a system with two quadcopters connected to the same power tether. Power supply readings from the experiments in various configurations are consistent with the predictions from the analysis (within 5%), which experimentally validates the presented analysis. A two-quadcopter system powered via a single tether is flown through a corridor to demonstrate one of the capabilities of having multiple quadcopters on the same tether.**

I. Introduction

Micro aerial vehicles like quadcopters are used in various applications, from surveillance to manipulation to exploring other planets [1], [2]. While these vehicles are primarily utilized for passive tasks such as surveillance [3] and photography [4], research groups and industries actively pursue aerial vehicles for manipulation tasks involving grasping/positioning [5], assembling/dismantling parts [6], or transporting payloads [7] using one or more vehicles. Quadcopters and other unmanned aerial vehicles present a unique ability to manipulate an object without any task-space restrictions.

However, the aerial vehicles are largely constrained in their flight time, payload capacity, etc., due to their limited hardware and power supply. Notably, the power demand is higher in applications involving manipulations in addition to flying. Understanding the various factors that influence the energy consumption in the quadcopters is an essential first step in improving the flight time and range.

Various innovations towards extending the flight time/range of the quadcopters have been explored. Methods such as swapping the batteries at a ground station [8] or replacing batteries in-flight using other quadcopters [9], [10] are shown to extend the flight times more than 4 times. Other methods such as using the batteries in multiple stages [11] have also demonstrated increased flight times. However, these systems can run out of power if not replaced in time and would require the quadcopters to land.

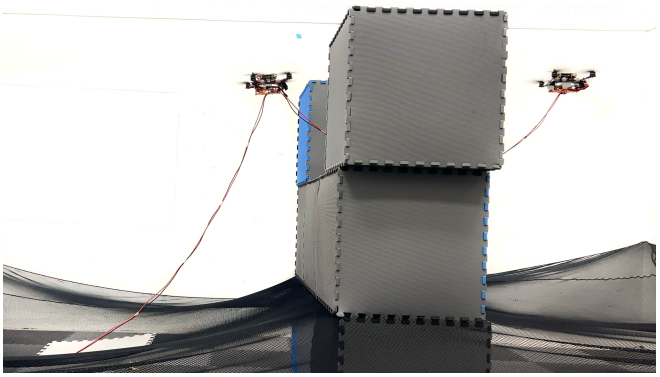

Fig. 1: Experiment demonstrating two quadcopters tethered using a single cable, supplying power from an external power source. The quadcopters are electrically connected in parallel. Multiple quadcopters can be used collaboratively to achieve tethered flight over unknown/challenging terrain while increasing the horizontal reachability of the quadcopter. Video for the experiment is provided as an attachment.

An alternate approach to extended flight time is to supply the power through an external tether from a fixed/mobile ground station. While a tethered quadcopter is limited in the flight range/maneuverability, in applications such as atmospheric analysis [12], construction/industrial inspections [13], surveillance [14], or aerial manipulation, the choice of tethering the quadcopter is a reasonable trade-off between maneuverability and extended flight. Their uses have also been demonstrated in a variety of commercial applications such as picking fruits in an orchard [15], and cleaning buildings and wind turbine blades. In this work, we study the tethered quadcopter system and analyze the different factors that influence the choice of power supply, tether parameters, etc.

A. Related Work

Tethered quadcopter systems to fixed or moving base have been explored in the in the past [16]–[19]. Control algorithms for the tethered quadcopters were developed in [20], where the tether is modeled as a massless rigid-link. This is assumption is valid for cases when the mass of the cable is significantly smaller than the thrusts generated by the quadcopter. To account for the mass of the cable during dynamic maneuvers, the tether is modeled as a series lumped mass links in [21]–[23]. Catenary models are used to model the tether in [24], [25], however can be used only under quasi-static conditions. In addition, a system of single

*denotes equal contribution and listed alphabetically.
†denotes equal advising contribution and listed alphabetically.
The authors are with the Dept. of Mechanical Engineering, UC Berkeley, CA 94720, USA. {karanjain, prasanth.kotaru, mz.desa, mwm, koushils}@berkeley.edu

tethered quadcopters have also been studied in [26], [27]. Most of the work in tethered quadcopters focus on modeling the system, and developing control and planning algorithms. Very few works look into power and energy analysis of the tethered power system.

Energy analysis for a downward tethered quadrotor is shown in [28]. However, the vehicle is not powered through the tether. Power supply for tethered drones is analyzed in [16], where comparisons between a battery operated drone and a tethered drone with external DC power source are drawn. However, the work doesn't look into the various factors that influence power consumption of tethered drone such as tether mass, resistance, input voltage etc.

B. Contributions

In this work, we look into tethered quadcopters powered trough the tether using an external power source. The contributions of this work are,

- We consider the different electrical and mechanical elements that influence the power consumption of a single tethered quadcopter under quasi-static hover conditions.
- We formulate the power consumption from the power source as a function of vehicle and cable masses, resistance, position of the quadcopter hover w.r.t to the fixed end of the tether, input voltage and predict the power required for a given setup.
- Analysis show existence of a critical height beyond which it is physically infeasible to hover the quadcopter .
- We present experimental results validating the analytical predictions.
- We demonstrate an application for multiple tethered quadcopters , flying through an corridor.

C. Organization

Rest of the paper is organized as follows. Section II describes the single tethered quadcopter system and provides a brief review into the dynamics of the system. Section III formualted the power consumption and power supply requirements for the tethered quadcopter system and discusses the analytical solutions. Finally, experimental results validating the analytical solutions is provided in Section IV. Concluding remarks are in Section V.

II. System Description

In this section, we describe a tethered quadrotor powered through the tether from an external source. We will briefly review the dynamics of the tethered quadcopters and present the catenary forces due to the tether under quasi-static conditions.

Consider a uniform tether supply connected to an external power source attached to a quadcopter as shown in Fig. 2. One end of the tether is attached to a quadcopter and the other is fixed to the ground at, say $\mathbf{x_0} \in \mathbb{R}^3$ in the inertial-frame. We assume the tether is rigidly attached to the center-of-mass of the quadcopter , i.e., the tether applies only translation force on the quadcopter .

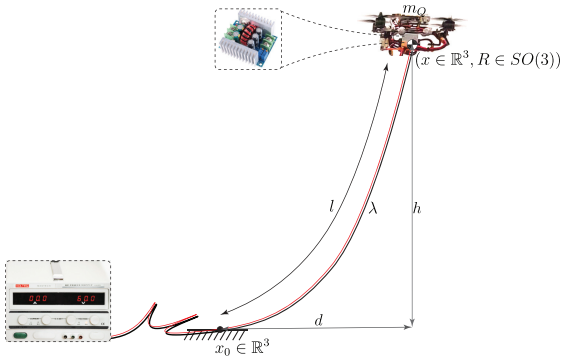

Fig. 2: Schematic of a tethered quadcopter flight with an external power source. An external high-voltage power supply is used to power the quadcopter . To reduce transmission power losses a step-down voltage converter is used onboard the quadcopter to step down the high source voltages to quadcopter operating voltages.

Variables	Definition
m_Q	Mass of the quadcopter [kg]
λ	Tether mass per unit length $[\mathrm{kg\,m^{-1}}]$
L	Total tether length [m]
l	Length of the tether in flight [m]
$\mathbf{x_0} \in \mathbb{R}^3$	Point of contact of the tether on the ground [m]
$\mathbf{x} \in \mathbb{R}^3$	Position of the quadcopter in the inertial-frame [m]
$R \in SO(3)$	Rotation from quadcopter-frame to inertial-frame
$\mathbf{\Omega}$	Angular velocity in body quadcopter -frame
$\{\mathbf{e_1}, \mathbf{e_2}, \mathbf{e_3}\}$	Inertial-frame basis vectors
$f \in \mathbb{R}$	Scalar thrust magnitude of the quadcopter [N]
$\mathbf{M} \in \mathbb{R}^3$	Moment of the quadcopter in the body-frame [N m]
$\mathbf{T} \in \mathbb{R}^3$	Force on the quadcopter due the tether in flight []
P_Q	Quadcopter Power consumption during hover [W]
ρ	Resistance of the tether per unit length $[\Omega\,\mathrm{m^{-1}}]$
V_s	Voltage at the source [V]
i_s	Current delivered by the source [A]
ΔV_s	Voltage drop across the tether [V]
$V_{b,in}, V_{b,out}$	Input and output voltage for the buck converter [V]

TABLE I: List of various mechanical and electrical variables used in this work.

The position of the center-of-mass of the quadcopter in the inertial-frame is $\mathbf{x} \in \mathbb{R}^3$. Define a body-fixed frame at the center of mass of the quadcopter and let $R \in SO(3)$ be the rotation from body-fixed frame to the inertial-frame. The mass and inertia-matrix (in body-frame) of the quadcopter are m_Q and J. Let the total length of the tether from the power source to the quadcopter be L, and let l be the length of the segment of the tether in flight. We assume the tether is uniform along its length, with λ mass per unit-length. Table I lists the various symbols used in this work.

The dynamics of the quadcopter with the tether with no external disturbances such as drag/wind can be summarized as follows,

$$m_Q \ddot{\mathbf{x}} = -m_Q g \mathbf{e_3} + f R \mathbf{e_3} + \mathbf{T}, \tag{1}$$

$$J\dot{\mathbf{\Omega}} = \mathbf{M} - \mathbf{\Omega} \times J\mathbf{\Omega}, \tag{2}$$

where, $f \in \mathbb{R}$ is the scalar thrust magnitude, $\mathbf{M} \in \mathbb{R}^3$ is the moment due to the propellers in the body-fixed frame, $\mathbf{\Omega}$ is the body angular velocity w.r.t. inertial-frame expressed in the body-frame, $\mathbf{e_3}$ is the axis pointing upward (opposite the direction of gravity). $\mathbf{T}$ is the force on the center-of-mass of the quadcopter by the attached tether.

A uniform cable suspended between two fixed-points

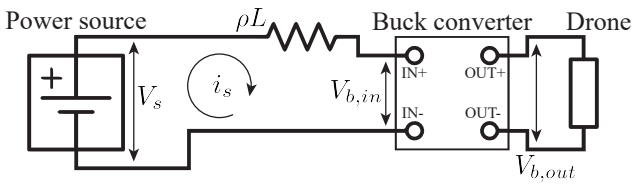

Fig. 3: Circuit diagram for the proposed power supply architecture for a tethered quadcopter. High voltage is used to transmit power via the tether to reduce resistive losses and a DC-DC step-down (buck) converter is attached to the quadcopter to bring the voltage down to a usable level by the quadcopter.

forms a catenary curve [29], where the catenary equation in a 2D plane using the catenary parameters a, b, c can be expressed as,

$$z = a \cosh\left(\frac{y-b}{a}\right) + c, \tag{3}$$

and can be numerically solved using the position of the end points. At hover, under quasi-static conditions, we can assume that the tether between the quadcopter takes the catenary shape. For tethers with no torsion, the catenary shape of the tether segment l lies in a vertical catenary plane, $\mathcal{C}$, between the points of suspension, $\mathbf{x_0}$ and $\mathbf{x}$. Let, $R_{\mathcal{C}}$ be the rotation from the catenary-plane to inertial-frame. Due to the symmetry in the tethered system, without loss of generality, we assume that the catenary plane $\mathcal{C}$ coincides with the $\mathbf{e_2 e_3}$ plane, at hover. Using the catenary equation (3) and quasi-static equilibrium condition, the tensions at the end points can be solved; Let,

$$\mathbf{T} = \boldsymbol{\tau}(h, d) = \bar{\boldsymbol{\tau}}(\mathbf{x_0}, \mathbf{x}), \tag{4}$$

where h and d are the horizontal and vertical distances of the quadcopter from the fixed end of the tether in the catenary plane $\mathcal{C}$. See Appendix A, for more details on computing the tensions.

For $h = l$ and $d = 0$ (when the quadcopter is vertically above the fixed point on the ground), the force due to the tether is the gravity on the segment of the tether in flight.

A typical quadcopter is powered using lithium polymer batteries. For the tether quadcopter, we supply the power from an external DC power source. The tether acts as the conductor to supply the power. A step-down voltage converter can be used onboard the quadcopter, depending on the power supply input.

In order to optimally design a power-supply system and to choose the type of tether for a tethered quadcopter flight, we need to understand the effect of various design parameters. Power required depends on the amount of thrust that the quadcopter is generating and is a function of the quadcopter position $\mathbf{x}$ and the position of the fixed end of the tether $\mathbf{x_0}$. Power consumption also depends on the maneuvers that the quadcopter is performing, thus for this work we restrict the flights to just hovers. In the next section, we analyze various electrical and mechanical parameters that influence power consumption of a tethered quadcopter at hover.

III. System Analysis

In this section, we analyze the power consumption and power supply requirements for a single quadcopter tethered to a power supply. In the first part of the section, we restrict the analysis to vertical flight. In a later part we analyze the effect of the horizontal component of the tether force. A schematic of the system explaining various parameters is shown in Fig. 2, and the circuit diagram is shown in Fig. 3.

A. In-flight power consumption by the quadcopter

The mass of the quadcopter m_Q includes all the components on the quadcopter excluding the tether. The mass per unit length of the tether λ includes both the live and neutral wire. The length of the portion of the tether in flight (not in contact with the ground) is l. At hover, we have the total thrust produced by the quadcopter in (1) as,

$$f = \|m_Q g \mathbf{e_3} - \mathbf{T}\|. \tag{5}$$

When the quadcopter is at hover vertically above $\mathbf{x_0}$, the total thrust equals the amount of force required to lift m_Q and tether mass λl,

$$f = (m_Q + \lambda l)\, g = mg, \tag{6}$$

Using the power analysis based on actuator disk model presented in [11], we claim that the electrical power consumption of the powertrain is,

$$P_Q = c_p m^{\frac{3}{2}} \tag{7}$$

where the power constant[a] c_p is a function of the propeller size A_{prop}, ambient air density ρ_{air}, gravity, propeller efficiency η_{prop} based on the propeller figure of merit, powertrain efficiency η_{pt}, and number of propellers n,

$$c_p = \frac{1}{\eta_{\text{prop}}\eta_{\text{pt}}} \sqrt{\frac{g^3}{2\rho_{\text{air}} n A_{\text{prop}}}} \tag{8}$$

We assume that the propeller and powertrain efficiency are constant and neglect power consumption by the onboard sensors and computers.

B. Electrical power supply analysis

The total length of the tether between the power supply and the quadcopter is L, also referred to as the "electrical length" of the cable. The resistance per unit length of the tether is taken to be ρ (again, this includes both the live and neutral wire). Therefore the resistance of the tether is ρL.

The power supply voltage and current are denoted as V_s and i_s respectively. The voltage drop across the tether then is $\Delta V_s = i_s \rho L$. Therefore, the input voltage and current at the buck converter is (see Fig. 3 for reference),

$$V_{b,in} = V_s - \Delta V_s = V_s - i_s \rho L \tag{9}$$

$$i_{b,in} = i_s \tag{10}$$

[a]For the same quadcopter system, the power constant is dependent on environmental factors such as air density and acceleration due to gravity. Therefore, c_p would be different in different environments such as other planets or moons. For example, on Mars the gravity is 38% that of Earth, and the air density is 1.7% that of Earth. As a result, the power constant is about 1.8× that on Earth. This means a tethered power supply would be very impactful on Mars since the batteries would deplete almost twice as fast as compared to on Earth.

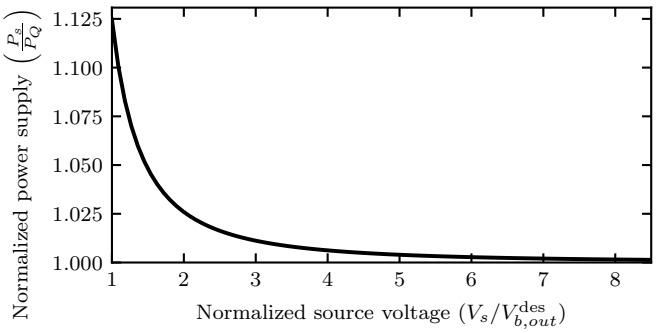

Fig. 4: Plot of source power P_s vs. source voltage V_s. The power is normalized by the electrical power consumption of the quadcopter P_Q, given everything else (hover height, tether parameters, etc.) is fixed. The source voltage is normalized by the desired input voltage to the quadcopter $V_{b,out}^{\text{des}}$.

The desired output voltage of the buck converter $V_{b,out}^{\text{des}}$ is set to a constant value by the user and the actual output voltage $V_{b,out}$ is approximately constant as long as $V_{b,in} > V_{b,out}^{\text{des}}$. If we assume the voltage conversion efficiency to be η_b, then the buck converter input and output parameters can be related as,

$$V_{b,out} i_{b,out} = \eta_b V_{b,in} i_{b,in} \tag{11}$$

Typically, the conversion efficiency is a function of the voltage conversion ratio $\frac{V_{b,out}}{V_{b,in}}$ and the power to be converted. However, for a given quadcopter system and hover height, the power required and the output voltage are fixed and therefore, we can assume η_b to be constant.

Note that the left hand side of (11) is the power input to the quadcopter P_Q at the end of the tether. We can substitute (7), (9) and (10) in (11) to get,

$$c_p \left(m_Q + \lambda l\right)^{\frac{3}{2}} = \eta_b \left(V_s - i_s \rho L\right) i_s \tag{12}$$

Note that all parameters in the above equation are either known via measurements and empirical data or are design parameters for a system, except for the power supply current i_s. Therefore, this formula can be used to predict the current output from power supply, and hence the power P_s from the power supply.

Equation (12) is a quadratic in i_s with two positive roots. Although both roots make physical sense, the higher root is not meaningful because it corresponds to a very high current flow that results in very high resitive losses leading to the same power delivered to the quadcopter as the lower root. Therefore, only the root with the lower value is considered.

For efficiency considerations and power supply limitations, the variable of interest is the power input from the power supply. So we convert the equation into a quadratic in P_s. The left-hand side of equation (12) is written in short-hand as $P_Q(\mathbf{x})$. With that notation, the quadratic is as follows,

$$\rho L P_s^2 - V_s^2 P_s + V_s^2 \frac{P_Q(\mathbf{x})}{\eta_b} = 0 \tag{13}$$

The meaningful solution in the fully expanded form is,

$$P_s = \frac{V_s^2}{2\rho L}\left(1 - \sqrt{1 - \frac{4\rho L c_p \left(m_Q + \lambda l\right)^{\frac{3}{2}}}{\eta_b V_s^2}}\right) \tag{14}$$

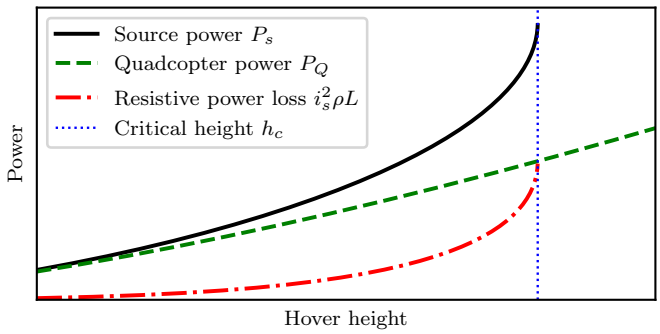

Fig. 5: Power supplied by the power source P_s and electrical power consumption by the quadcopter P_Q vs. hover height of the quadcopter h (with the tether vertically down), assuming $\eta_b = 1$. For a specific configuration, it is not physically possible to hover the quadcopter beyond the critical height h_c. Note that the power supply requirement is still finite at the critical height. The limit arises because any additional current from the power supply adds to the resistive losses and does not get delivered as useful power to the quadcopter.

C. Supplied power vs. source voltage

Increasing V_s arbitrarily does not arbitrarily decrease P_s. As $V_s \to \infty$, we have $\Delta V_s \to 0$, but the power source still needs to supply the power required by the quadcopter . In an ideal case, where the above limits are reached and we have an ideal buck converter with 100% efficiency, the power supplied vs. input voltage would look as shown in Fig. 4.

In practical scenarios however, the efficiency of the buck converter depends on the conversion ratio, switching frequency, power converted, etc [30]. As a result, depending on the parameters, there would typically be an optimal input voltage at which we minimize the power supplied.

D. Supplied power vs. wire gauge

The values of mass and resistance per unit length for different wire gauges are manufacturer dependent and are not explicitly known *a priori*. However, for a given manufacturer, we can assume a general trend for resistance and mass. With decreasing wire gauge, the mass of the tether decreases and the resistance increases. This information, in general is not enough to predict the behavior of power supplied vs. the wire gauge used because the dependence on the parameters ρ and λ is nonlinear and complex as can be seen in (14). Empirical values are calculated in Section IV to get insight on these trends.

E. Supplied power vs. quadcopter hover height

In this subsection, we consider quadcopter hovering with the tether vertically down i.e. mechanical length of the cable lifted by the quadcopter l is simply equal to the height h at which the quadcopter is flying. The electrical length is still fixed to L. Note that in equation (14), the term inside the square root is strictly decreasing with $l = h$. Therefore, it will reach zero at some critical quadcopter height h_c, beyond which the power source will be unable to provide enough power for the quadcopter to hover – this is because any increase in current will increase the resistive losses and not enough power will be left to meet the demand of the quadcopter . We would like to emphasize that this

is not a limitation of the power source, but of the tether-quadcopter system because of the physical parameters such as resistance and power consumption requirements. The critical height can be computed as follows,

$$0 = 1 - \frac{4\rho L c_p \left(m_Q + \lambda h_c\right)^{\frac{3}{2}}}{\eta_b V_s^2} \tag{15}$$

$$\implies \eta_b V_s^2 = 4\rho L c_p \left(m_Q + \lambda h_c\right)^{\frac{3}{2}} \tag{16}$$

$$\implies h_c = \frac{1}{\lambda}\left[\left(\frac{\eta_b V_s^2}{4\rho L c_p}\right)^{2/3} - m_Q\right] \tag{17}$$

If the height at which the resistive losses overwhelm the fundamental power supply limit exceeds the electrical length L of the tether, then we can fly at any location allowed under the mechanical limits imposed by the tether, which are analyzed further in Section III-F. However, for the other case we need to be careful when choosing the hover height since the electrical limits forbid the quadcopter to hover above this critical height even if the tether's mechanical limits allow it. Note that when flying at the critical height, the resistive power loss is exactly half the power supplied by the source. A sample plot for supplied power, quadcopter power consumption and resistive power losses vs. hover height is shown in Fig. 5.

The critical hover height essentially determines the reach of our system and some applications might require a high hover height. One of the simplest ways to increase this is by increasing the supply voltage V_s and using the appropriate voltage converter at the quadcopter to step-down to the quadcopter 's rated voltage. This is analogous to what power grids do to minimize losses over the transmission lines.

An interesting case arises when the critical height is same as the tether length – this allows us to maximize the possible hover height, given everything else (supply voltage, masses, etc.) is held constant. We will call this the critical length $L_c = h_{c,\max}$. Starting from (16), we can derive,

$$L_c^2 \left(m_Q + \lambda L_c\right)^3 = \frac{\eta_b^2 V_s^4}{4\rho^2 c_p^2 g^3} \tag{18}$$

This is a fifth-order polynomial in L_c, which does not have a closed-form solution. Numerical values for our system are calculated in the experimental validation section.

F. Supplied power vs catenary forces

In the previous section, we analyzed the power required for a vertical flight of a tethered quadcopter system. However, from (5), at hover, the total thrust required by the quadcopter depends on the catenary force $\mathbf{T}$ which in turn depends on how far the quadcopter is from the fixed end on the ground. Therefore the power required/supplied are function of the quadrotor position (h, d) in the vertical plane. Given the two ends of the tether, at hover, the shape of the catenary can be computed by solving the catenary equation (4). The tension directions at the end are computed by solving for the gradient of the catenary equation. Finally, the catenary forces are solved for at quasi-static equilibrium, as shown in Appendix A. The net thrust generated by the quadrotor in (5) is converted to augmented mass as,

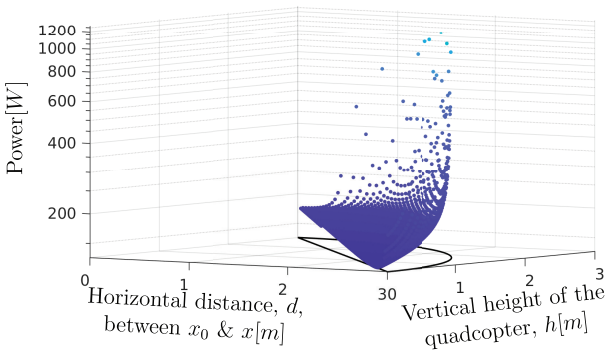

Fig. 6: Analytical prediction of the source power using (19) and (14). The power required and tension in the tether reach arbitrarily large values as the tether reaches its physical length limit.

$$\bar{m} = \frac{f}{g} = \frac{\|m_Q g \mathbf{e_3} - \mathbf{T}\|}{g}. \tag{19}$$

The augmented mass $\bar{m}$ is used to compute the power consumption on the quadcopter using (7) as,

$$P_Q = c_p \bar{m}^{\frac{3}{2}}. \tag{20}$$

Finally, using (14), we have the power requirement from the source for catenary systems. Fig. 6 shows the power supply P_s as function of height h and distance from the fixed end of the tether d. As seen in the figure, P_s increases asymptotically to infinity towards the physical limit of the tether, i.e, an arbitrarily large force is required to fully extend the tether. This corresponds to the asymptotic case where the catenary curve is a straight line.

IV. Experimental Validation

In this section, we present the experimental validations for the analyses presented in the previous section. In the later part of the section, we present a system with two quadcopters connected mechanically in series, using a single tether that supplies the power to both the quadcopters from an external DC power supply. Note that electrically, the two quadcopters are connected in parallel to ensure that both operate at the rated voltage.

A. Setup

The experiments are conducted in an indoor flight-space equipped with a motion capture system for position and attitude tracking. Custom-build quadcopters are used to test the tethered hover flights. The quadcopters are equipped with current & voltage sensors to measure the onboard readings. A low-pass filter is applied to the current and voltage readings and the power consumed by the quadcopter is computed from these readings. We use silicone insulated electric wire of length $L = 7.62\,\mathrm{m}$ for tethered power supply, and a $1200\,\mathrm{W}$, high voltage ($60\,\mathrm{V}$ maximum), high current ($20\,\mathrm{A}$ maximum) DC power supply to power the quadcopters. For supply voltages higher than $12.6\,\mathrm{V}$ (operating voltage for the BLDC motors used in the quadcopters), commercially available step-down DC converters (buck converters) are installed on the quadcopters to step-down voltages to $12.6\,\mathrm{V}$.

Wire Gauge	$\lambda\,[\mathrm{kg\,m^{-1}}]$	$\rho\,[\Omega\,\mathrm{m^{-1}}]$	Diameter [mm]
10 AWG	0.142	0.01299	2.588
12 AWG	0.095	0.01659	2.053
14 AWG	0.055	0.02408	1.628

TABLE II: Properties of the silicone insulated electric wires used as power supply tether in the experiments.

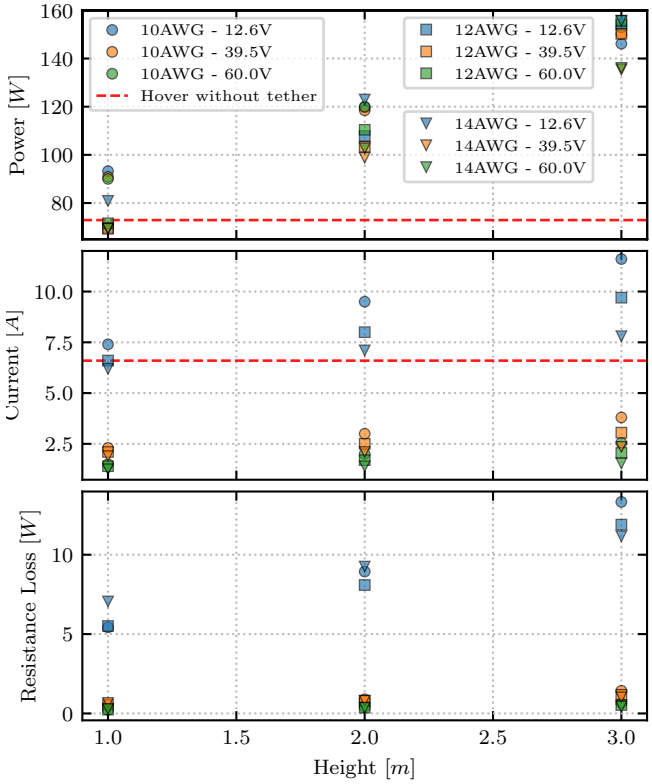

Fig. 7: Power measured at the external DC power source vs. hover height of the quadcopter (with the tether vertically down), for different input voltages and wire gauges.

B. Single tethered quadcopter at hover vs. design factors

We compare the power consumption of a tethered quadcopter, with the tether suspended vertically down, against three different design factors. Hover flight experiments with the tether suspended vertically down are conducted to compute the power, for different wire sizes, input voltages and heights. Physical properties of the different tethers are listed in Table II. The mass of the quadcopter m_Q is maintained constant across all the tests.

Power and current readings measured at the input source are given in Fig. 7. As shown in the figure, the power measured for the tethered flights as expected (due to the additional tether mass) is higher than a nominal quadcopter flight using a battery. As seen from Table II, the mass per unit-length of 10AWG[b] tether is higher than the rest, this results in a higher power consumption for 10AWG tether as evident from the figure.

Experimental hover videos for all the different design factors are shown in the video attachment.

[b]American Wire Gauge. More information about wire parameters for different gauges can be found on `https://wikipedia.org/wiki/American_wire_gauge`

C. Predictions from Analysis

We calculate values from formulae derived in the analysis to compare with experimental values. The power constant for the quadcopter used for this particular set of experiments is calculated to be $c_p = 144.538\,\mathrm{W/kg^{3/2}}$ from previous empirical data. The tether length used is $L = 7.62\,\mathrm{m}$. Since there are a lot of input design variables, we present values only for 12AWG tether at $12.6\,\mathrm{V}$ (arbitrarily chosen).

For hover heights of $\{1.0, 2.0, 3.0\}\mathrm{m}$, the predicted power supplied P_s values are $\{81.95, 102.15.124.57\}\mathrm{W}$. The experimental values for the supplied power are $\{83.16, 100.80, 122.22\}\mathrm{W}$. We can see that the values match pretty well with less than a 5% error across all comparisons, which includes values for the other wire sizes and supply voltages.

We can also compute the critical height and length for the 12AWG wire at $12.6\,\mathrm{V}$ supply using (17) and (18). For a tether length of $7.62\,\mathrm{m}$, the critical height is $h_c = 11.77\,\mathrm{m}$. In this case, $h_c > L$, so the quadcopter can fly anywhere mechanically allowed by the tether. The critical length is computed to be $L_c = 9.43\,\mathrm{m}$. This is the maximum height the quadcopter can hover at, and is only possible when the tether length is chosen to be the critical length.

D. Effect of catenary forces on the power

In the section, we run hover experiments using 10AWG tether at $l = 3.0\,\mathrm{m}$, fixed on an elevated platform as shown in Fig. 8. We run the hover tests at various points along the circle, in the vertical plane, with increasing horizontal distance d. An input supply of $12.6\,\mathrm{V}$ is provided to the system, and $c_p = 150.175\,\mathrm{W/kg^{3/2}}$ for the quadcopter is empirically determined. Experimental power consumption is compared to the analytical results predicted using (19) and (14). The catenary forces are solved using (4) (see Appendix A for details).

As in the figure, the analytical predictions are close to the actual experimental results. While, the commanded set-points are along the circle of radius l, the quadcopter stabilized to smaller circle of $2.839\,\mathrm{m}$ radius. As discussed in Section III-F, the power required increases asymptotically to infinity as we get closer to the physical length limit of the tether. We compute the analytical power required at the points along the radius $2.839\,\mathrm{m}$, shown in Fig. 8 [top]. Power required increases with the increasing horizontal distance, due to the increase in the horizontal component of the catenary forces, before sharply dropping. This is due the decrease in the vertical component of the catenary force, as some of the vertical force required to lift tether is shared by the fixed end of the tether.

E. Two quadcopters connected on the same power tether

In this experiment, we use two quadcopters connected to a single tether (same power source), electrically connected in parallel to ensure similar operating voltage. A two quadcopters tethered system offers the same advantage as a single tethered quadrotors, such as extended flight time, steady external power supply. In addition, a two quadcopters system

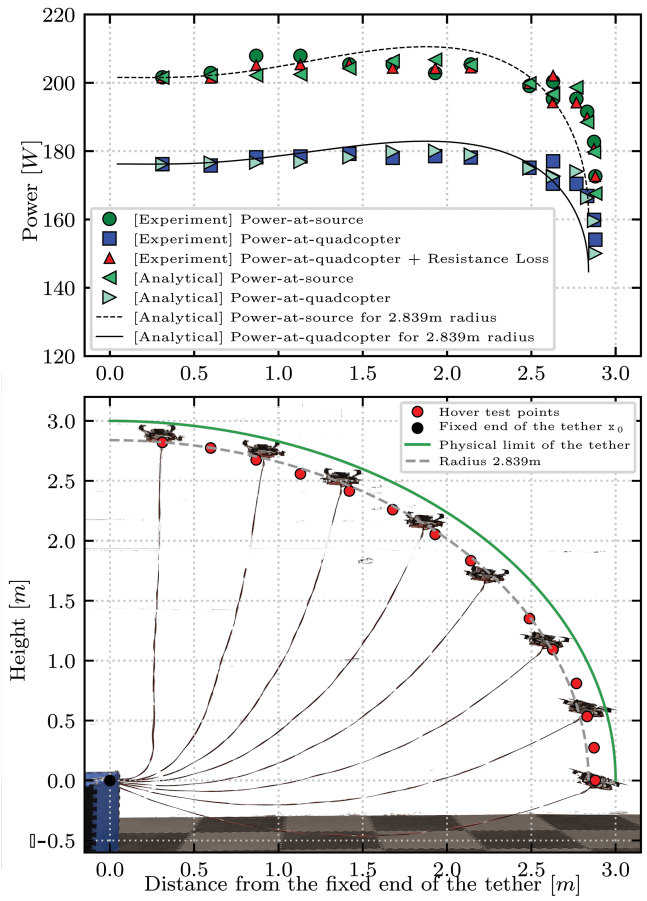

Fig. 8: [Top] Experimental and analytical power values at the source and the quadcopter. The power increases with increasing horizontal force before sharply dropping off when some of the vertical force required to lift tether is shared by the fixed end of the tether. Predicted power supply (dashed line) and predicted quadcopter power consumption along the radius 2.839 m (solid line) are also plotted. [Bottom] Visualization of the hover test points; Green line shows the physically reachable limit of the tether

can be used for a better horizontal reachability as shown in Fig. 1 that can operate over clutter or challenging terrain without endangering the supply tether. An experiment demonstrating the two quadcopters passing through a corridor is provided in the video attachment.

.

V. Conclusion and Future Work

In this paper, we have presented an analysis for a tethered quadcopter system to estimate the electrical power consumption by the quadcopter and the power supply requirement to deliver the desired power to the quadcopter, for different configurations of the tether. The analysis includes various mechanical, aerodynamic and electrical parameters of the tether-quadcopter system. We discovered that there is a critical hover height for any tethered-quadcopter system beyond which it is fundamentally impossible for the quadcopter to hover regardless of how much power we can supply. We have also presented an analysis for the catenary forces, quadcopter thrust and power supply requirement for different configurations of the system.

The power supply analysis is then experimentally validated by flying the quadcopter at different heights, supplying various voltages from the power supply, and using three different wire sizes. The catenary force and power analysis is also expeirmentally verified by flying the quadcopter at different desired locations and measuring the attitude, thrust and power consumption. Experimental values match well (within 5%) with the predicted values from the analyses which confirms that the assumptions used in the analyses are realistic.

Lastly, we show a system with two quadcopters powered using the same tether and demonstrate the better horizontal reachability it offers over a single tethered-quadcopter. An additional advantage offered by this system is performing distributed tasks that need quadcopters to operate in proximity such as picking fruits or cleaning a high-rise building.

An extension to this work is to extend the power supply analysis to the system of multiple quadcopters on the same tether. This will allow users to spec the power supply and tether sizes optimally for their specific system. Another extension is to explore what happens when flying close to the critical height described in the paper. Other advantages and limitations for multiple quadcopters on a single tether can also be explored.

Acknowledgment

We gratefully acknowledge financial support from 42air and the Chang-Lin Tien Graduate Fellowship. The experimental testbed at the HiPeRLab is the result of contributions of many people, a full list of which can be found at `hiperlab.berkeley.edu/members/`.

References

[1] H. F. Grip, J. Lam, D. S. Bayard, D. T. Conway, G. Singh, R. Brockers, J. H. Delaune, L. H. Matthies, C. Malpica, T. L. Brown *et al.*, "Flight control system for nasa's mars helicopter," in *AIAA Scitech 2019 Forum*, 2019, p. 1289.

[2] R. D. Lorenz *et al.*, "Dragonfly: A rotorcraft lander concept for scientific exploration at Titan," *Johns Hopkins APL Technical Digest*, vol. 34, no. 3, p. 14, 2018.

[3] A. Jaimes, S. Kota, and J. Gomez, "An approach to surveillance an area using swarm of fixed wing and quad-rotor unmanned aerial vehicles UAV(s)," in *2008 IEEE International Conference on System of Systems Engineering*. IEEE, 2008, pp. 1–6.

[4] E. Cheng, *Aerial photography and videography using drones*. Peachpit Press, 2015.

[5] J. Fishman, S. Ubellacker, N. Hughes, and L. Carlone, "Dynamic grasping with a" soft" drone: From theory to practice," in *2021 IEEE/RSJ International Conference on Intelligent Robots and Systems (IROS)*. IEEE, 2021, pp. 4214–4221.

[6] F. Augugliaro, S. Lupashin, M. Hamer, C. Male, M. Hehn, M. W. Mueller, J. S. Willmann, F. Gramazio, M. Kohler, and R. D'Andrea, "The flight assembled architecture installation: Cooperative construction with flying machines," *IEEE Control Systems Magazine*, vol. 34, no. 4, pp. 46–64, 2014.

[7] P. Kotaru, G. Wu, and K. Sreenath, "Differential-flatness and control of multiple quadrotors with a payload suspended through flexible cables," in *IEEE Indian Control Conference (ICC)*, Kanpur, India, January 2018, pp. 352–357.

[8] D. Lee, J. Zhou, and W. T. Lin, "Autonomous battery swapping system for quadcopter," in *2015 international conference on unmanned aircraft systems (ICUAS)*. IEEE, 2015, pp. 118–124.

[9] K. P. Jain and M. W. Mueller, "Flying batteries: In-flight battery switching to increase multirotor flight time," in *2020 IEEE International Conference on Robotics and Automation (ICRA)*. IEEE, 2020, pp. 3510–3516.
[10] K. P. Jain, M. Park, and M. W. Mueller, "Docking two multirotors in midair using relative vision measurements," *arXiv preprint arXiv:2011.05565*, 2020.
[11] K. P. Jain, J. Tang, K. Sreenath, and M. W. Mueller, "Staging energy sources to extend flight time of a multirotor uav," in *2020 IEEE/RSJ International Conference on Intelligent Robots and Systems (IROS)*. IEEE, 2020, pp. 1132–1139.
[12] D. A. Rico, F. Muñoz-Arriola, and C. Detweiler, "Trajectory selection for power-over-tether atmospheric sensing uas," in *2021 IEEE/RSJ International Conference on Intelligent Robots and Systems (IROS)*. IEEE, 2021, pp. 2321–2328.
[13] K. Watanabe, K. Kinoshita, I. Nagai, and M. K. Habib, "Development of a camera-mounted tethered quadrotor for inspecting infrastructures," in *IECON 2016-42nd Annual Conference of the IEEE Industrial Electronics Society*. IEEE, 2016, pp. 6128–6133.
[14] A. J. Torgesen, J. P. How, and B. Cameron, "Airborne sensing for ship air wake surveys with a tethered autonomous uav," in *AIAA Scitech 2021 Forum*, 2021, p. 0381.
[15] Y. Maor, E. Shifman, and E. Moshe, "Device and method for fruit harvesting," Sep. 16 2021, uS Patent App. 17/200,965.
[16] W. Walendziuk, D. Oldziej, and M. Slowik, "Power supply system analysis for tethered drones application," in *2020 International Conference Mechatronic Systems and Materials (MSM)*. IEEE, 2020, pp. 1–6.
[17] L. Zikou, C. Papachristos, and A. Tzes, "The power-over-tether system for powering small uavs: Tethering-line tension control synthesis," in *2015 23rd Mediterranean Conference on Control and Automation (MED)*. IEEE, 2015, pp. 681–687.
[18] M. Tognon, S. S. Dash, and A. Franchi, "Observer-based control of position and tension for an aerial robot tethered to a moving platform," *IEEE Robotics and Automation Letters*, vol. 1, no. 2, pp. 732–737, 2016.
[19] M. Tognon and A. Franchi, *Theory and Applications for Control of Aerial Robots in Physical Interaction Through Tethers*. Springer Nature, 2020, vol. 140.
[20] M. M. Nicotra, R. Naldi, and E. Garone, "Taut cable control of a tethered uav," *IFAC Proceedings Volumes*, vol. 47, no. 3, pp. 3190–3195, 2014.
[21] T. Lee, "Geometric controls for a tethered quadrotor uav," in *2015 54th IEEE conference on decision and control (CDC)*. IEEE, 2015, pp. 2749–2754.
[22] P. Kotaru and K. Sreenath, "Multiple quadrotors carrying a flexible hose: dynamics, differential flatness and control," *IFAC-PapersOnLine*, vol. 53, no. 2, pp. 8832–8839, 2020.
[23] P. Kotaru, G. Wu, and K. Sreenath, "Differential-flatness and control of quadrotor (s) with a payload suspended through flexible cable (s)," in *2018 Indian Control Conference (ICC)*. IEEE, 2018, pp. 352–357.
[24] D. S. D'antonio, G. A. Cardona, and D. Saldaña, "The catenary robot: Design and control of a cable propelled by two quadrotors," *IEEE Robotics and Automation Letters*, vol. 6, no. 2, pp. 3857–3863, 2021.
[25] V. Abhishek, V. Srivastava, and R. Mukherjee, "Towards a heterogeneous cable-connected team of uavs for aerial manipulation," in *2021 American Control Conference (ACC)*. IEEE, 2021, pp. 54–59.
[26] B. Kosarnovsky and S. Arogeti, "A string of tethered drones-system dynamics and control," in *2019 European Conference on Mobile Robots (ECMR)*. IEEE, 2019, pp. 1–6.
[27] M. Bolognini and L. Fagiano, "Lidar-based navigation of tethered drone formations in an unknown environment," *IFAC-PapersOnLine*, vol. 53, no. 2, pp. 9426–9431, 2020.
[28] C. Lee, J. J. Son, H. Lee, and S. Han, "Energy consumption analysis of downward-tethered quadcopter," in *2021 21st International Conference on Control, Automation and Systems (ICCAS)*. IEEE, 2021, pp. 1212–1215.
[29] E. H. Lockwood, *A book of curves*. Cambridge University Press, 1967.
[30] J. Gragger, A. Haumer, and M. Einhorn, "Averaged model of a buck converter for efficiency analysis." *Engineering letters*, vol. 18, no. 1, 2010.

APPENDIX A

Determining the Catenary Parameter: The catenary equation for the catenary curve in the $\mathcal{C}$ is given in (3). WLOG let y, z be the e_2 and e_3 component of a vector in the inertial plane, i.e.,

$$y_0 = \mathbf{x_0} \cdot \mathbf{e_2}, z_0 = \mathbf{x_0} \cdot \mathbf{e_3}, y = \mathbf{x} \cdot \mathbf{e_3}, == \mathbf{x} \cdot \mathbf{e_3} \quad (21)$$

For the suspended cable system, we define three constraints, vertical and horizontal distances between the two attachment points (y_0, z_0) and (y, z), and tether length l. Evaluating an arc length integral $\int(\sqrt{1+\frac{dz}{dy}^2})dy = l$ between the endpoints of the catenary curve, we obtain the constraint,

$$l = a\sinh(\tfrac{y-b}{a}) - a\sinh(\tfrac{y_0-b}{a}). \quad (22)$$

Vertical distance between the end points is,

$$h \coloneqq z - z_0 = a\cosh(\tfrac{z-b}{a}) - a\cosh(\tfrac{z_0-b}{a}), \quad (23)$$

and $d := y - y_0$. Finally, using a hyperbolic identity, we solve for a,

$$\sqrt{l^2 - h^2} = 2a\sinh^2(\tfrac{d}{2a}). \quad (24)$$

(24) is transcendental equation and is solved numerically. The parameters b and c are then computed as follows,

$$b = \tfrac{y0+y}{2} - a\tanh^{-1}(h/l), c = z_0 - a\cosh(y_0 - b)/a. \quad (25)$$

Solving for Tension: The direction of the tensions at the end points are defined by the gradient of the catenary curve at the end point. Unit $2D$ gradients at the end points in the catenary plane $\mathcal{C}$ is given as,

$$\nu_0 = \tfrac{1}{(\sinh^2(z_0/a)+1)^{1/2}} \begin{bmatrix} 1 & \sinh(z_0/a) \end{bmatrix}^T \quad (26)$$

$$\nu = \tfrac{1}{(\sinh^2(z/a)+1)^{1/2}} \begin{bmatrix} 1 & \sinh(z/a) \end{bmatrix}^T. \quad (27)$$

At quasi-static equilibrium, the net-forces on the tether balance out, thus the tension magnitude at the end points can be computed using,

$$t_0\nu_0 + t\nu = \begin{bmatrix} 0 \\ mg \end{bmatrix}. \quad (28)$$

Finally the tether force on the quadrotor in $\mathcal{C}$ is given by $t\nu$.